SATURATION EXPONENT IN LOW PERMEABILITY SANDSTONE BY POROUS PLATE AND CENTRIFUGE DESATURATION METHODS

Joel D. Walls, Rock Physics Associates
Marilyn Black, Core Laboratories
Carol Admire, formerly with Core Laboratories

Abstract

This paper will focus on the laboratory methods of measuring resistivity index on tight gas sand samples. This process is of great importance because the values of saturation exponent, N, which are measured on cores have a large effect on the log calculated water saturation. We have chosen to investigate the two most common methods of saturation change for tight gas sand resistivity index testing. These are the porous plate method and the centrifuge method. Because of the low permeability of tight gas sands, the centrifuge method is by far the least time consuming. However, it is commonly assumed that the porous plate method always produces more even saturation distribution and more accurate N values than the centrifuge method. Using an x-ray scanning method, we have found that at lower S_W, the centrifuge and the porous plate method both produce relatively constant saturation along the length of the sample.

Tight gas sand samples are unique in several respects that are relevant to desaturation and resistivity measurement at partial saturation. First, there is no oil present and the samples are strongly water wet. Second, the low permeability and small pore throat size cause a relatively steep capillary pressures curve, so that a small saturation gradient produces a large pressure gradient. This means that there is a strong tendency for saturation gradients to disappear, but this tendency is likely retarded to some extent by the small permeability to water at lower water saturations.

Four samples from the Travis Peak Formation and two from the Frontier Formation were tested. The macroscopic fluid distribution (saturation versus position along the sample) is most strongly affected by desaturation method at the higher S_W's. In particular, the centrifuge method caused higher S_W near the outflow end of the sample for most total saturations above about 50%. However, our results show that the method used to reduce saturation does not have a large effect on the calculated N when all saturations are averaged together. The data obtained shows that N values measured with the centrifuge method are valid for log interpretation purposes in tight gas sands.

Research Objectives

The research objectives were;

- Determine effects of porous plate and centrifuge desaturation methods on saturation distribution in tight sands.
- Determine effects of porous plate and centrifuge desaturation methods on saturation exponent in tight sands.

Experimental Procedures

Centrifuge and Porous Plate Desaturation Comparison

The samples chosen for this work include four depths from the Travis Peak Formation, SFE #3 well and two depths from the Frontier Formation, Enron S. Hogsback well. The samples had been cleaned and dried during previous special core analysis testing. We chose to use non-preserved samples because we were primarily interested in the effects of fluid distribution and the method of desaturation on N.

We first placed the dry samples in a x-ray scanning system and measured beam intensity versus position along the sample. Next, we obtained the dry porosity and grain density of the samples and then they were placed in a high pressure saturating vessel. We applied a vacuum of about 0.001 atm. for 12 hours and then flooded the vessel with degassed brine. The brine was composed of 68,000 PPM NaI (R_W=0.2 Ohm-m) to improve x-ray attenuation. We applied a pressure of 2000 PSI to the brine for 24 hours to achieve 100% saturation of the samples. After saturation, the samples were again placed in the x-ray scanning system. The difference between the fully saturated and dry scan intensity was calculated at each position, for each sample.

All samples were marked with orientation lines so that the sample was mounted in the x-ray system in the same position each time. To correct for variations in the beam intensity, an aluminum section of the same diameter as the core was placed on each end of the sample. The beam scanned aluminum first, then the sample, then aluminum again. This all occurred within about 2 minutes, so the intensity of the beam could be normalized with great accuracy. A schematic diagram of the x-ray scanning system is shown in Figure 1. The width of the x-ray beam windows and the geometry of the scanning system gives a linear resolution 0.063" (4% of sample length). About 80% of the sample volume was scanned. We believe this is adequate to measure relative water saturation along the length of the sample.

We measured electrical resistivity by two terminal and four terminal methods using silver current and potential electrodes (see Figure 2). In this paper the words "terminal" and "electrode" have the same meaning. The electrical frequency was 1000 Hz. The measurements were made at ambient temperature (22° to 25° C). A thermocouple was used to measure the temperature of each sample to ±0.1° C. The resistivity of each sample was corrected to 25° C using Arp's equation. The samples were 1.5" in diameter by 1.5" to 2" in length. The external hydrostatic confining pressure (P_c) was 4200 PSI and the pore pressure (P_p) was 500 PSI during the formation factor measurements. This produced a net confining stress (P_{net}) of 3700 PSI which was approximately equal to the in-situ net overburden pressure.

After formation factors were measured, the fully saturated samples were weighed and placed in a high speed centrifuge where water saturation was reduced to about 85%. They were removed from the centrifuge and reweighed to precisely determine saturation for the entire sample. After one hour they were scanned with the x-ray system and placed into the core holder for resistivity index (RI) measurement at 3700 PSI net stress and ambient pore pressure. The scan and RI measurement were repeated after 24 hours of equilibrium. During times when the samples were out of the core holder, they were carefully wrapped in Saran™ plastic film and stored in a humidified chamber to prevent fluid evaporation. Water saturation versus position was calculated by comparing the partial saturation scan data to the dry and fully saturated scan data, assuming beam attenuation was linearly dependant on the NaI brine saturation. The x-ray scanning was used to observe saturation gradients, but all the N values were calculated from the gravimetric saturations.

The process of centrifugation, scanning and RI was repeated at target saturations of 60%, 50%, 40% and residual water saturation, S_{wr}. We arbitrarily defined S_{wr} as the lowest saturation that a sample would achieve after 8 hours in the centrifuge at the highest speed that would not damage the sample. Travis Peak samples were subjected to higher speeds than Frontier samples because they were stronger. Therefore they generally have lower S_{wr}'s by centrifuge than the Frontier samples. Following the centrifuge desaturation tests, the samples were leached in methanol, dried at 85° C for 48 hours in a convection oven and then cooled to room temperature. We remeasured porosity, saturated the samples and remeasured the formation factor.

Resistivity index was then determined at multiple partial water saturations, obtained by placing the samples in a cell capillary pressure apparatus and desaturating by displacement with gas. The porous plate was a ceramic material with a 15 bar bubble point pressure. After the desired saturation was obtained, the samples were removed from the cell, weighed, scanned, and resistivity index was measured by two and four electrode methods. We used the same target saturations as in the centrifuge tests, except that S_{wr} was the lowest brine saturation that could be obtained with the 15 bar gas displacement pressure allowed by the ceramic plate.

Results

Effect of Equilibrium Time

For centrifuge desaturation there is little difference between resistivity of the samples 1 hour after spin compared to 24 hours after spin. This is supported by the saturation distribution plots, which show relatively little redistribution of fluid over a 24 hour time period. The distribution profile for Travis Peak (SFE #3) sample 7384.0 after centrifuge desaturation is shown for an example (Figure 3). In this plot, the left side of the x axis is the downstream end of the sample and the right side of the x axis is the upstream end of the sample. The downstream end was against the outer circumference of the centrifuge during centrifuge desaturation and was against the porous plate during porous plate desaturation. The thin horizontal dashed lines show the average water

saturation for the sample determined by weight. The vertical heavy lines show the position of the potential electrodes on the sample. These electrodes were one inch apart for all four samples. The resistivity index for the centrifuge desaturation run (1 hour and 24 hour equilibrium) is shown in Figure 4. The porous plate saturation profile for sample 7384.0 is shown in Figure 5 and the resistivity index plot is shown in Figure 6. The resistivity index and saturation exponent data are presented in Tables 1 and 2.

Using centrifuge desaturation (Figure 4), the four terminal N value for this sample, after 1 hour of equilibrium time at each saturation, was 1.41. After 24 hours of equilibrium at each saturation, the value was 1.38. At the higher two average water saturations, there was a substantial variation of S_w versus position which was partially removed by the additional equilibrium time. For example, at 56% S_w, the saturation near the outflow end (left side of plot) dropped from about 80% to 66% between 1 hour and 24 hours.

With the porous plate desaturation method (Figure 6), the four terminal saturation exponent was 1.35 after 1 hour and 1.41 after 24 hours. Since the N values have an experimental uncertainty of about ±0.05, these changes are not considered significant. There is a possibility that further equilibrium time could have evened out the saturation distribution and caused changes in N. However, tests run on other samples for periods up to 100 hours have indicated little or no change after 24 hours.

Effect of Desaturation Method on Fluid Distribution and N

In this section, we examine the differences between saturation profiles and N values resulting from porous plate versus centrifuge desaturation. All data were taken after 24 hours of equilibrium time at each saturation level.

Travis Peak Samples (SFE #3 Well)

Saturation exponents, N, by centrifuge ranged from 1.16 to 1.38 by the four electrode method. Saturation exponents by porous plate ranged from 1.25 to 1.41 which compares very favorably to the centrifuge results. Tables 1 and 2 show resistivity index and saturation exponents of the four samples by centrifuge and porous plate techniques, respectively. The agreement between the porous plate and centrifuge results is encouraging but the N values were considerably less than reported by Luffel, Herrington, and Walls (1993) on samples from the same depths. We believe that the lower N's may be related to a different brine formulation (68,000 PPM NaI) which was used in the second set of tests.

Saturation distribution and resistivity index plots for all four Travis Peak samples after 24 hours of equilibration are shown in Figures 7 through 13. For each sample there are two plots, one for centrifuge desaturation and one for porous plate desaturation. Each figure shows saturation distribution along the length of the sample, the corresponding resistivity index versus brine saturation and the single point N versus brine saturation. Two and four electrode results are shown for all samples. Two electrode data are measured over the entire length of the sample. Four electrode resistivity data are measured between the potential electrodes which are denoted by heavy vertical lines labeled P.E. on the saturation distribution plots.

These plots show some interesting results in terms of the water saturation distribution and its effect on resistivity. It is usually assumed that centrifuge desaturation produces higher water saturation at the outflow end of the sample because water is displaced in that direction by the centrifugal force. Similarly, it is usually assumed that the porous plate desaturation process produces relatively constant saturation gradients. Both of these assumptions are predicated on the sample being homogeneous along its length. The data in these tests indicate that three of the four samples may have been inhomogeneous.

Sample 7382.5 exhibits a slightly decreasing S_w toward the outflow end of the sample following centrifuge desaturation (CD) at most average S_w's except 45%. Following porous plate desaturation (PPD), the sample shows considerably lower S_w at the outflow end of the sample for all S_w's. S_w seems to be slightly more evenly distributed at the lower average S_w's. Also, S_w tends to be more evenly distributed in the centrifuge case than in the porous plate case.
The considerably different saturation distribution between CD and PPD has a fairly minor effect on saturation exponent, which is obtained by fitting a straight line through all of the resistivity

index data. For sample 7382.5, the greatest difference between the CD and PPD N values is at 24 hour equilibrium and with four electrodes. PPD produced a N of 1.18 while CD produced a N of 1.31. This may be caused by the large variation in S_W in the porous plate case. For example, at 22% average S_W, the saturation varies from about 15% to 28% between the potential electrodes. The saturation distributions which occurred in this sample indicate that the outflow end may have had larger pore sizes which desaturated more than the rest of the sample.

Sample 7384 produced more even saturation distributions than 7382.5, but there is a reduction in S_W at the upstream end of the sample for the lower S_W's in the porous plate desaturation case which may be related to sample inhomogeneity. As discussed in Section 2, this sample had higher S_W at the outflow end in the centrifuge case at 56% average S_W which resulted from the centrifuge displacement process. The higher S_W at the downstream end does not occur at lower average S_W's indicating that capillary forces within the sample are acting to offset the centrifuge forces. All saturation exponent results for this sample are about 1.4 (± 0.05), again indicating that the process of calculating N from a linear least squares fit of all of the S_W data tends to mask the effects which are occurring at individual S_W's.

Like the previous samples, 7388.8 has higher S_W's at the downstream end resulting from the CD process. This effect tends to show up mostly at the intermediate S_W's. Porous plate S_W's are fairly evenly distributed for this sample, which appears to be the most homogeneous of the four. Two electrode and four electrode N values differ by about 0.1 with the 2 terminal values being greater. The reason for this difference is not apparent in terms of saturation distribution, so it is probably caused by high contact resistance in the two electrode case. The CD process produced a slightly lower N than the PPD process for this sample, even though saturation gradients are small in both cases. Sample 7390.5 has the most uneven saturation distribution of the four samples, particularly in the PPD case. We feel that this unusual distribution is due to the inclined bedding planes which exist in this sample. The bedding planes may be acting to retain more water on the downstream end of the sample. As with sample 7388.8, this sample has a lower saturation exponent from CD than from PPD.

Frontier Formation (Enron South Hogsback Well)

Data for the Frontier Formation samples are presented in Tables 3 and 4. Plots of the centrifuge and porous plate data after 24 hours equilibrium for samples 7114.2 and 7127.5 are shown in Figures 15 to 18. Two electrode resistivity is measured over the entire length of the sample. Four electrode resistivity is measured between the potential electrodes. In both cases, saturation is plotted as the average saturation for the whole sample, determined gravimetrically. The N values were calculated by fitting a straight line to the log of RI vs. log of S_W data. These values, with porosity and cementation exponent, M, are shown in the small box in the far bottom right of each figure. The saturation exponent versus saturation plots (right side of figures), show the trend of N as saturation changes.

For sample 7114.2, there is little difference between the average N values from porous plate and centrifuge desaturation. This is probably because the saturation distributions for both desaturation methods are also very similar. For sample 7127.5, the centrifuge desaturation N values are about 0.1 higher than the porous plate values. This difference may not be significant because there is an uncertainty in these results of about plus or minus 0.05. For sample 7127.5, the porous plate saturation distribution is more even across the length of the sample at the higher S_W's. The centrifuge saturation distribution shows higher S_W's at the outflow end of the sample due to the centrifugal force acting in that direction. Notice that this effect is absent at the two lower S_W's. We believe this happens because the capillary pressure, which acts to redistribute the saturation is very high at these saturation levels. In both samples and with both desaturation methods, there is a trend of increasing N with decreasing S_W. Also, there is greater difference between the two and four electrode results at the higher saturations and this difference diminishes as the saturation goes lower.

Discussion of Results

A possible explanation for the difference in resistivity between porous plate and centrifuge desaturation may be related to microscopic or pore scale saturation distribution. The plots of N versus brine saturation in Figures 7 through 18 are provided to show that N tends to increase with

decreasing S_w in these samples, but the effect seems to be more pronounced with porous plate desaturation than with centrifuge desaturation. Worthington and Pallatt (1990) suggested an explanation of this effect in terms of increasing tortuosity as S_w decreases. This increase may not always produce a linear increase of RI versus S_w on log-log coordinates. With multi-modal pore throat distributions the tortuosity may increase in a manner which causes N to increase with decreasing S_w. Worthington stated that this effect might be likely in microporous rock. If large enough, this effect could more than offset the effect of capillary-bound water which can cause lower N values at lower S_w (Givens and Schmidt, 1988). High pressure mercury injection tests indicate that pores with throats less than 0.0025 microns comprise 5 to 18% of the pore volume in samples from the Travis Peak and Frontier Formations.

The difference between centrifuge and porous plate resistivity index may result from differences in the way pores are interconnected in the two cases. Centrifugal force acts on each water molecule in a direction parallel to the sample axis. This may encourage connectivity of pores that are parallel to the sample axis and hence to the electrical current flow path. The capillary displacement method would allow for a more tortuous path of connected pores, since the controlling factor in desaturation is pore throat radius. Pores connected by pathways parallel to current flow, as the centrifuge may produce, could provide less resistance and cause lower RI values at a given S_w than they would if desaturated by the porous plate method.

However, this difference in saturation distribution is only speculation and we have no independent means to verify it. The average N values, when all saturations are considered, are quite similar between the porous plate and centrifuge methods (Table 5). The samples that were desaturated by centrifuge have quite flat saturation profiles at the lower S_w's. This result is contrary to those shown by Baldwin and Yamanashi (1989) for centrifugally desaturated Bedford limestone and Berea sandstone, where a significant saturation gradient was observed after equilibrium times of 5 to 6 days. The saturation gradients from the porous plate tests are also quite small and show no major changes with time. This result is contrary to the data of Sprunt et.al. 1991 for mixed wettability carbonates. The major difference with our experiments is probably the strong water wetness and higher capillary pressure in the tight sandstone which acts to limit the fluid saturation gradient. Based on this data, we believe that the results obtained from previous centrifuge desaturation tests (GRI Coop wells and SFE's 1,2, 3, and 4) are acceptable and useful for well log interpretation purposes.

Conclusions

1. Saturation distribution and saturation exponent are nearly the same 1 hour and 24 hours after centrifuge or porous plate desaturation.
2. Saturation distribution at the lower S_w values appears to be controlled more by sample heterogeneity than by the method used to desaturate.
3. Saturation distribution at the higher S_w values is more uneven for centrifuge desaturation than for porous plate desaturation.
4. Saturation exponent is about the same with porous plate and centrifuge desaturation.

References

Baldwin, B.A., and W.S. Yamanashi; Persistence of Nonuniform Brine Saturation Distribution in SCA Electrical Resistivity Study Core Plugs after Desaturation by Centrifuge, The Log Analyst, January-February, 1989, pp. 45-48.

Givens, W.W., and E.J. Schmidt; A Generic Electrical Conduction Model For Low-Contrast Resistivity Sandstones, SPWLA 29th Annual Logging Symp., San Antonio TX, June 5-8, 1988

Luffel, D.L., K. Herrington, and J.D. Walls; Effect Drying on Travis Peak Cores Containing Fibrous Illite, SPE Advanced Technology Series, April, 1993.

Sprunt, E.S., K.P. Desai, M.E. Coles, R.M. Davis, and E.L. Muegge; CT-Scan-Monitored Electrical Resistivity Measurements Show Problems Achieving Homogeneous Saturation, SPE Form. Eval., Vol. 6 No. 2, page 134, June, 1991.

Worthington, P.F., and N. Pallatt; Effect of Variable Saturation Exponent Upon the Evaluation of Hydrocarbon Saturation, SPE Paper 20538, Presented at the 65th Annual Technical Conference, New Orleans, LA, Sept 23-26, 1990.

Table 1: Resistivity Index and Saturation Exponent
Well: SFE #3, Centrifuge Desaturation
Net Confining Stress 3700 PSI, Frequency 1000 Hz, 25° C

Sample	Sat'n (%)	1 Hour Equilibrium Time				24 Hour Equilibrium Time			
		RI (2T)	RI (4T)	N (2T)	N (4T)	RI (2T)	RI (4T)	N (2T)	N (4T)
7382.5	100.0	1.00	1.00	1.32	1.34	1.00	1.00	1.32	1.31
	81.7	1.21	1.22			1.32	1.31		
	44.1	2.60	2.69			2.70	2.76		
	34.4	3.62	3.85			3.65	3.57		
	27.7	4.44	4.53			5.02	5.00		
	18.2	10.53	10.68			11.21	10.78		
7384	100.0	1.00	1.00	1.42	1.41	1.00	1.00	1.41	1.38
	80.5	1.31	1.36			1.34	1.35		
	56.3	1.94	1.87			1.97	2.05		
	38.9	3.55	3.56			3.49	3.51		
	34.0	3.97	3.96			4.41	4.22		
	22.7	9.01	8.84			9.08	8.53		
7388.8	100.0	1.00	1.00	1.31	1.21	1.00	1.00	1.28	1.16
	81.2	1.25	1.13			1.31	1.20		
	51.8	2.10	1.91			2.17	2.00		
	43.8	2.65	2.43			2.60	2.26		
	36.6	3.37	3.02			3.50	2.96		
	21.6	7.77	6.93			7.99	6.97		
7390.5	100.0	1.00	1.00	1.24	1.22	1.00	1.00	1.20	1.18
	79.3	1.33	1.33			1.31	1.27		
	57.9	1.77	1.76			1.71	1.83		
	38.7	2.89	2.86			2.93	2.79		
	34.8	3.14	2.94			3.32	3.32		
	22.3	7.05	6.96			6.88	6.54		

Table 2: Resistivity Index and Saturation Exponent
Well: SFE #3, Porous Plate Desaturation
Net Confining Stress 3700 PSI, Frequency 1000 Hz, 25° C

Sample	Sat'n (%)	1 Hour Equilibrium Time				24 Hour Equilibrium Time			
		RI (2T)	RI (4T)	N (2T)	N (4T)	RI (2T)	RI (4T)	N (2T)	N (4T)
7382.5	100.0	1.00	1.00	1.33	1.26	1.00	1.00	1.24	1.18
	66	1.64	1.67			1.68	1.51		
	53.3	1.94	1.80			1.83	1.76		
	48.3	2.70	2.36			2.50	2.23		
	29.6	4.43	4.09			4.34	4.08		
	20.8	8.05	7.64			7.59	7.36		
7384	100.0	1.00	1.00	1.4	1.35	1.00	1.00	1.44	1.41
	84.7	1.17	1.17			1.10	1.13		
	55.0	1.87	1.83			1.83	1.75		
	46.3	2.86	2.83			2.60	2.53		
	37.8	3.65	3.39			3.69	3.57		
	28.5	6.36	6.07			8.37	8.54		
7388.8	100.0	1.00	1.00	1.36	1.28	1.00	1.00	1.35	1.25
	66.8	1.68	1.57			1.75	1.64		
	52.2	2.40	2.18			2.14	1.95		
	47.1	2.49	2.25			2.69	2.36		
	32.1	4.81	4.65			5.04	4.80		
7390.5	100.0	1.00	1.00	1.35	1.28	1.00	1.00	1.36	1.35
	82.4	1.21	1.16			1.27	1.20		
	54.8	1.89	1.72			1.90	2.05		
	48.7	2.79	2.37			2.70	2.63		
	38.3	3.16	2.74			3.29	3.19		
	31.9	5.25	5.18			5.73	5.57		

Table 3: Resistivity Index and Saturation Exponent; Frontier Fm

Well: Enron South Hogsback, Centrifuge Desaturation
Net Confining Stress 2400 PSI, Frequency 1000 Hz, 25° C

Sample	Sat'n (%)	1 Hour Equilibrium Time				24 Hour Equilibrium Time			
		RI (2T)	RI (4T)	N (2T)	N (4T)	RI (2T)	RI (4T)	N (2T)	N (4T)
7114.2	100.0	1.00	1.00	1.66	1.53	1.00	1.00	1.77	1.60
	85	1.31	1.23			1.29	1.21		
	75	1.60	1.55			1.61	1.45		
	60	2.56	2.37			2.53	2.35		
	51	2.95	2.73			3.32	3.05		
7127.5	100	1.00	1.00	1.70	1.72	1.00	1.00	1.69	1.64
	84	1.29	1.48			1.29	1.16		
	72	1.70	1.77			1.70	1.77		
	55	2.61	2.65			2.70	2.68		
	47	3.65	3.53			3.75	3.55		

Table 4: Resistivity Index and Saturation Exponent; Frontier Fm

Well: Enron South Hogsback, Porous Plate Desaturation
Net Confining Stress 2400 PSI, Frequency 1000 Hz, 25° C

Sample	Sat'n (%)	1 Hour Equilibrium Time				24 Hour Equilibrium Time			
		RI (2T)	RI (4T)	N (2T)	N (4T)	RI (2T)	RI (4T)	N (2T)	N (4T)
7114.2	100	1.00	1.00	1.90	1.79	1.00	1.00	1.76	1.66
	85	1.29	1.17			1.23	1.15		
	74	1.64	1.55			1.7	1.61		
	61	2.71	2.34			2.53	2.33		
	44	4.64	4.58			4.29	4.14		
7127.5	100	1.00	1.00	1.70	1.65	1.00	1.00	1.59	1.54
	77	1.39	1.37			1.27	1.55		
	65	1.95	1.90			1.41	1.37		
	53	3.03	2.94			1.65	1.57		
	38	5.16	4.98			1.62	1.59		

Table 5: Saturation Exponents from Porous Plate and Centrifuge RI Tests; Four Electrode.

Sample	Formation	Centrifuge	Porous Plate
7382.5	Travis Peak	1.31	1.18
7384.0	Travis Peak	1.38	1.41
7388.8	Travis Peak	1.16	1.25
7390.5	Travis Peak	1.18	1.35
7114.2	Frontier	1.60	1.66
7127.5	Frontier	1.64	1.54
	Average	**1.38**	**1.40**

Figure 1: X-ray scanning system diagram

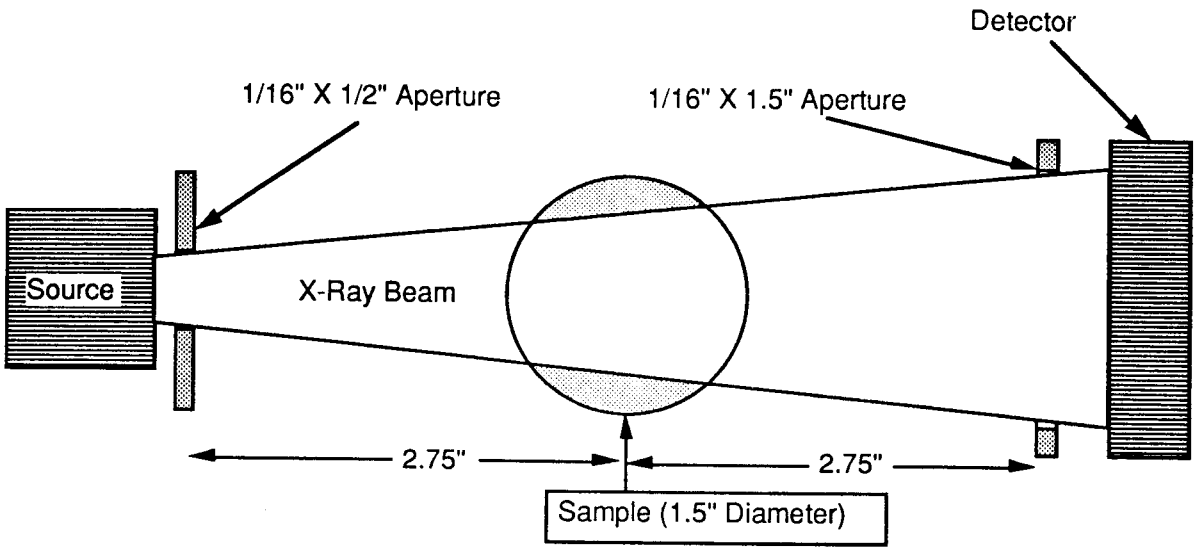

Saturation is measured in un-shaded area of sample cross-section (80% of total).

Figure 2: Schematic of four electrode measurement system.

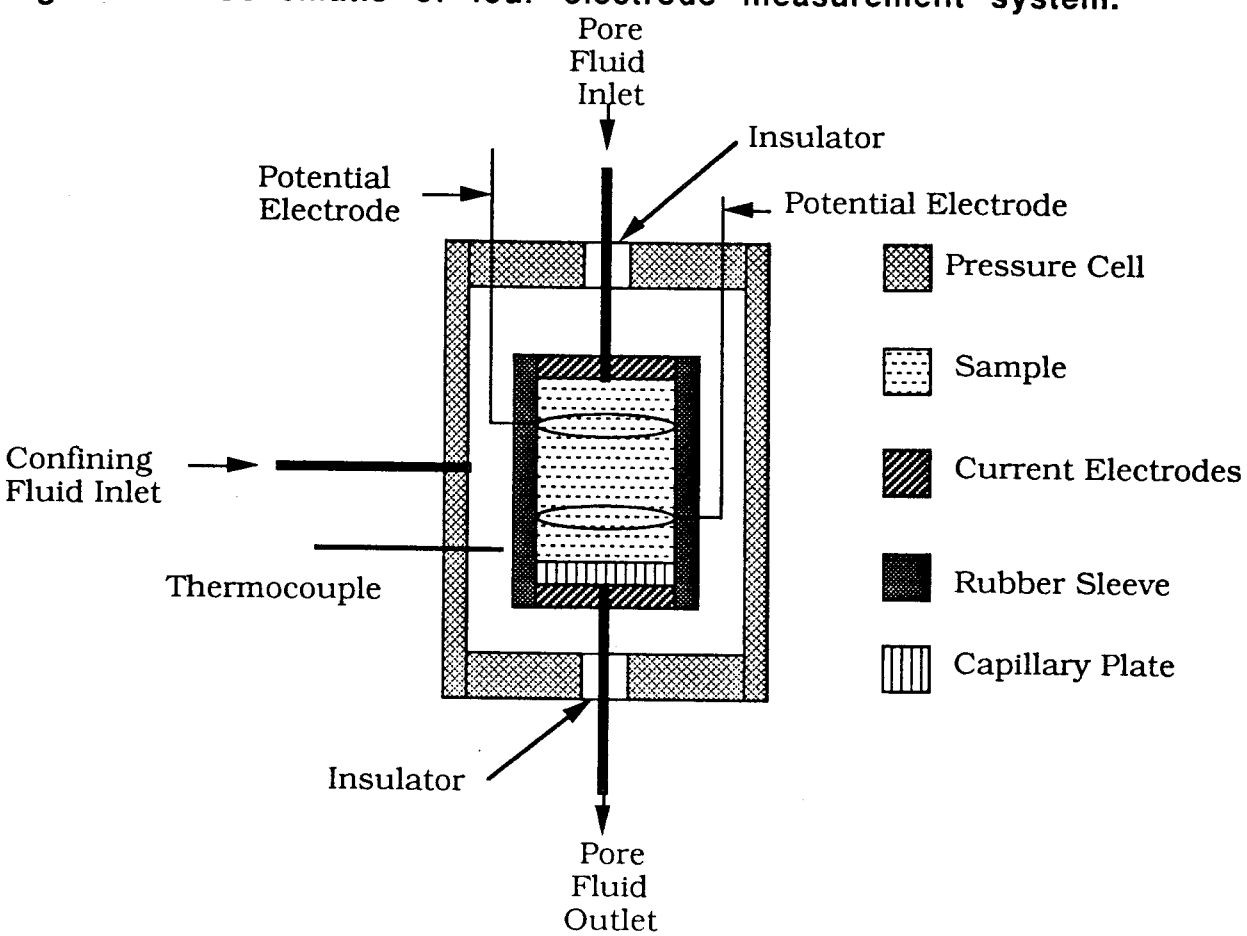

FIG. 3: Brine Saturation vs. Position: Sample 7384.0, Centrifuge Desat., 1 and 24 Hours Equilibrium Time

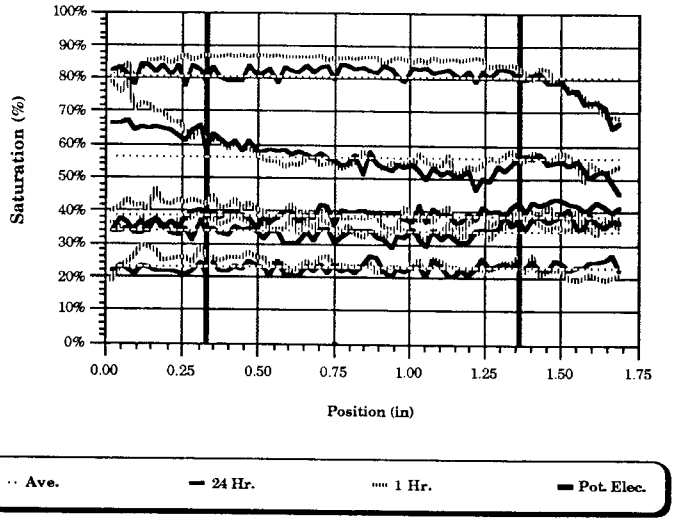

Figure 4: Resistivity Index vs. Saturation, Well SFE #3, Depth 7384, Centifuge Desat., 4-term, 1hr. and 24 hr. Equilibrium

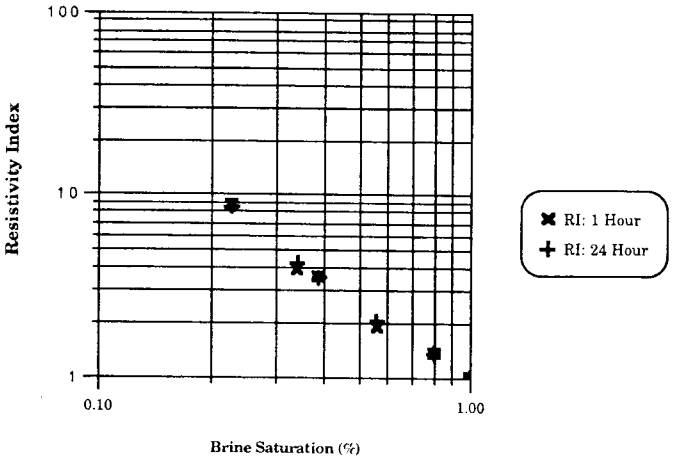

FIG. 5: Brine Saturation vs. Position: Sample 7384.0, Porous Plate Desat., 1 and 24 Hours Equilibrium Time

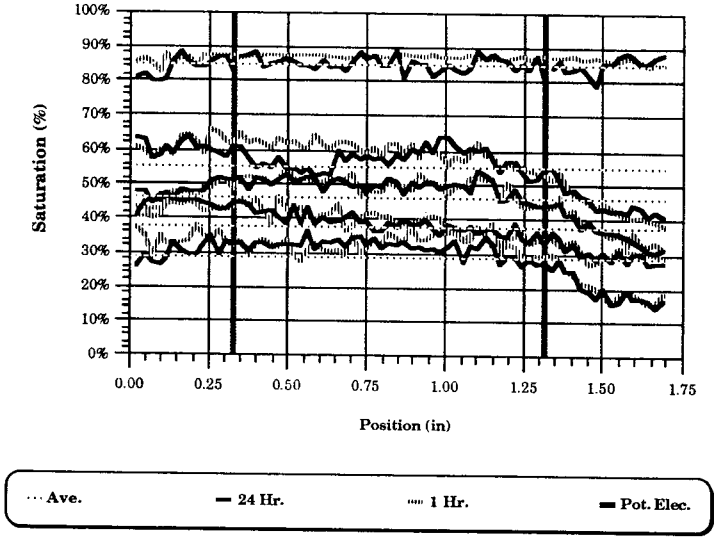

Figure 6: Resistivity Index vs. Saturation, Well SFE #3, Depth 7384, Porous Plate Desat., 4-term, 1hr. and 24 hr. Equilibrium

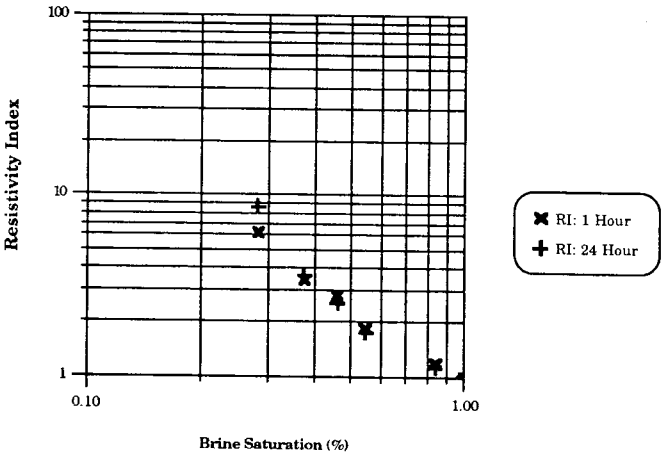

1993 SCA Conference Paper Number 9307

Figure 7: RI, N, and Sat. Dist., Sample 7382.5, Cent. Desat, 24 Hr.

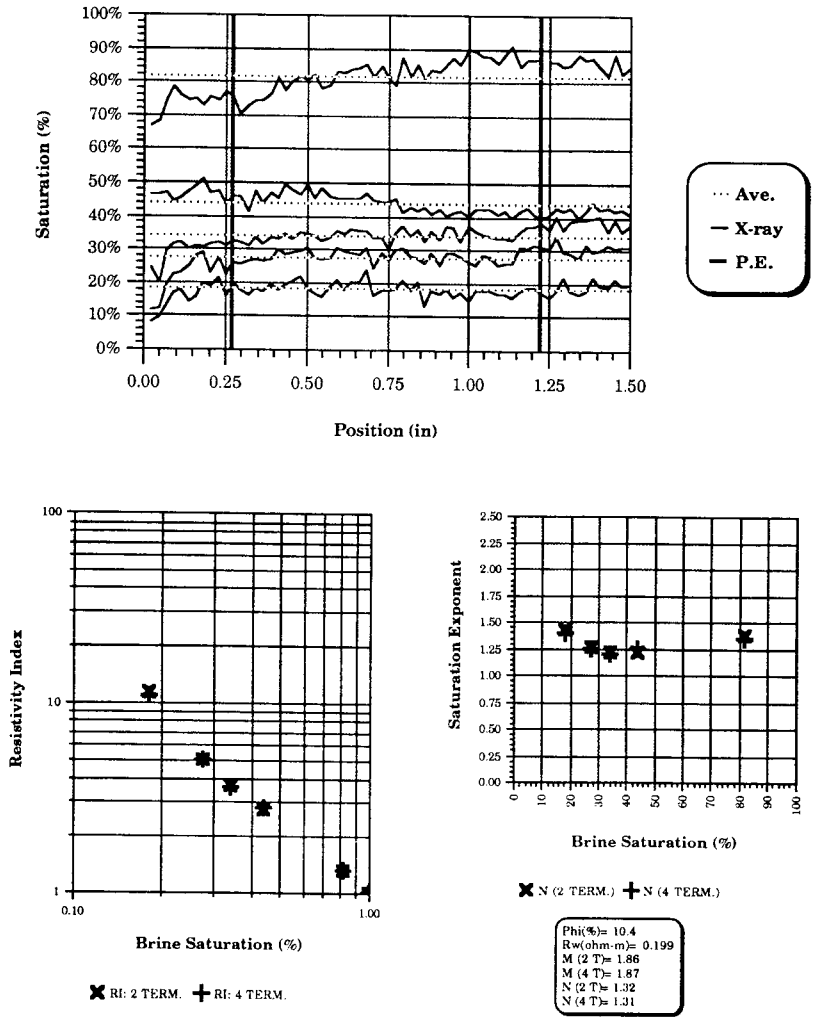

Figure 8: RI, N, and Sat. Distribution, Sample 7382.5, Porous Plate Desat., 24 Hr.

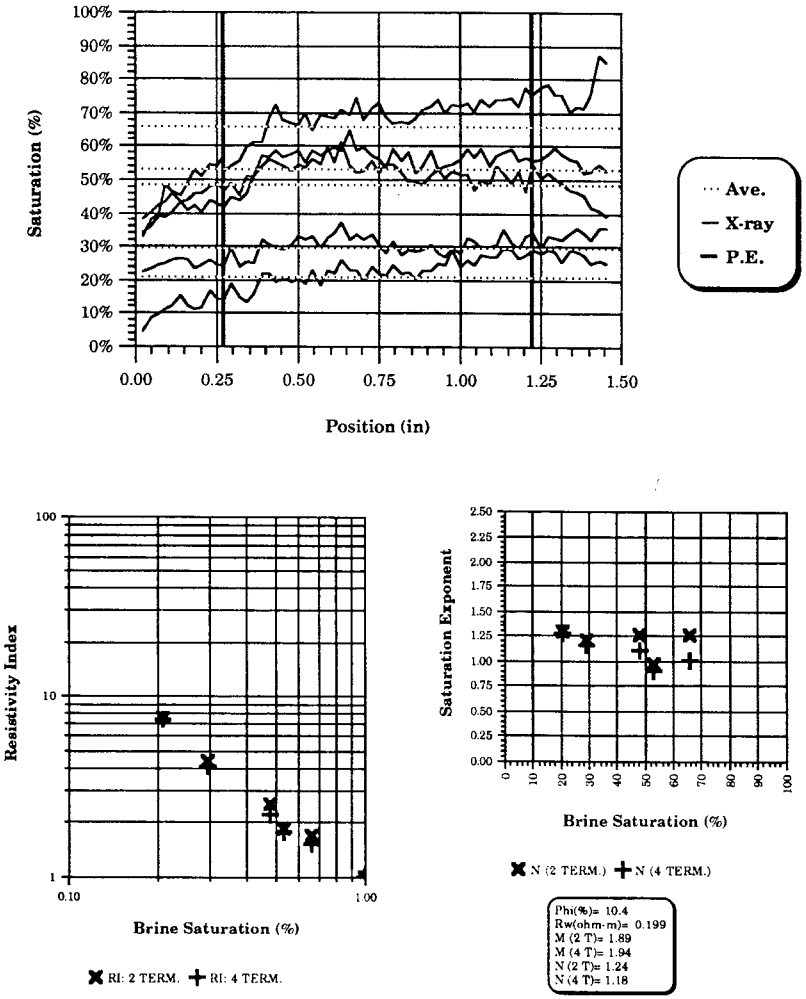

1993 SCA Conference Paper Number 9307

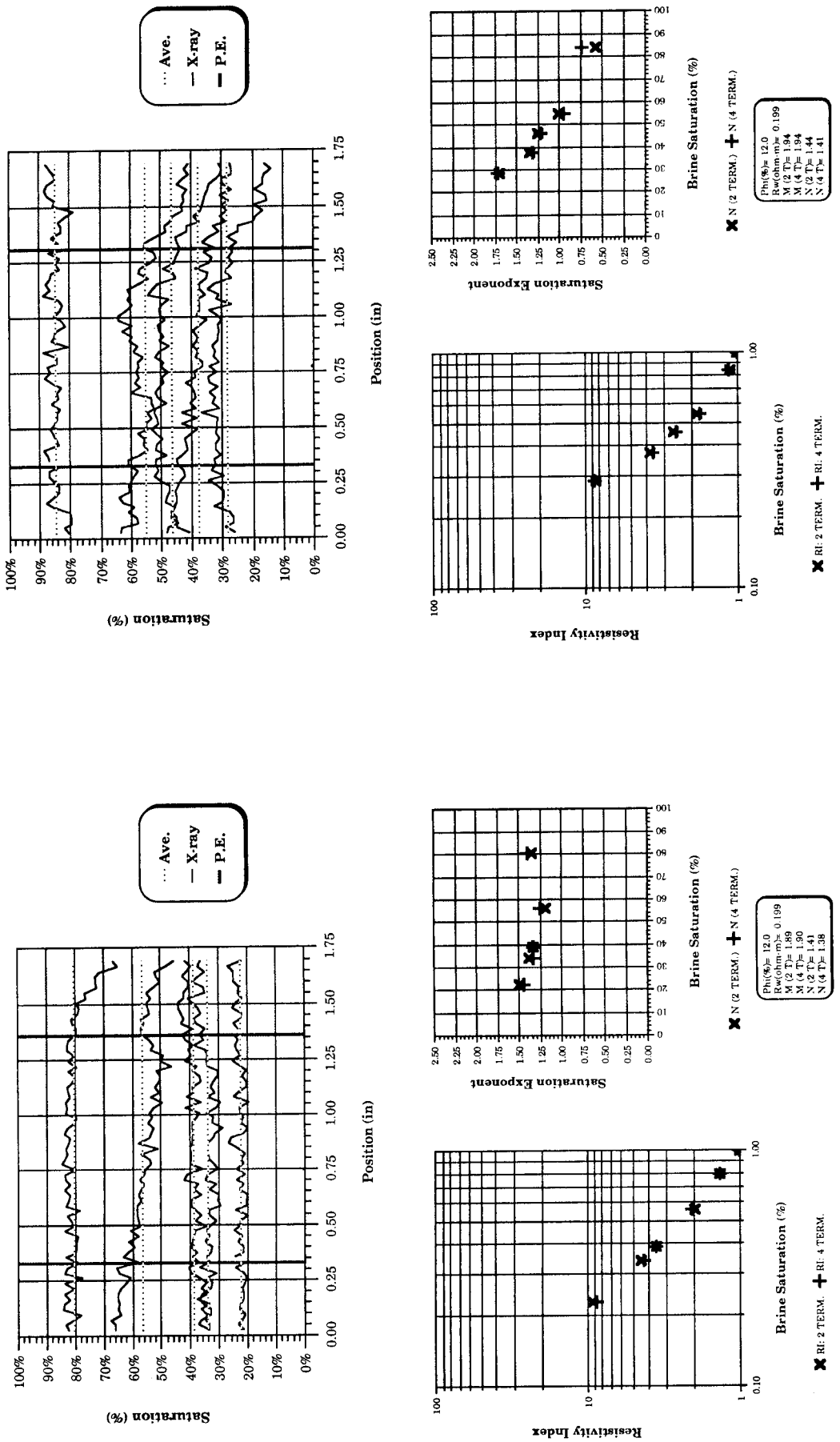

Figure 9: RI, N, and Sat. Dist., Sample 7384.0, Cent. Desat., 24 Hr.

Figure 10: RI, N, and Sat. Distribution, Sample 7384.0, Porous Plate Desat., 24 Hr.

Figure 11: RI, N, and Sat. Dist., Sample 7388.8, Cent.Desat.,24Hr.

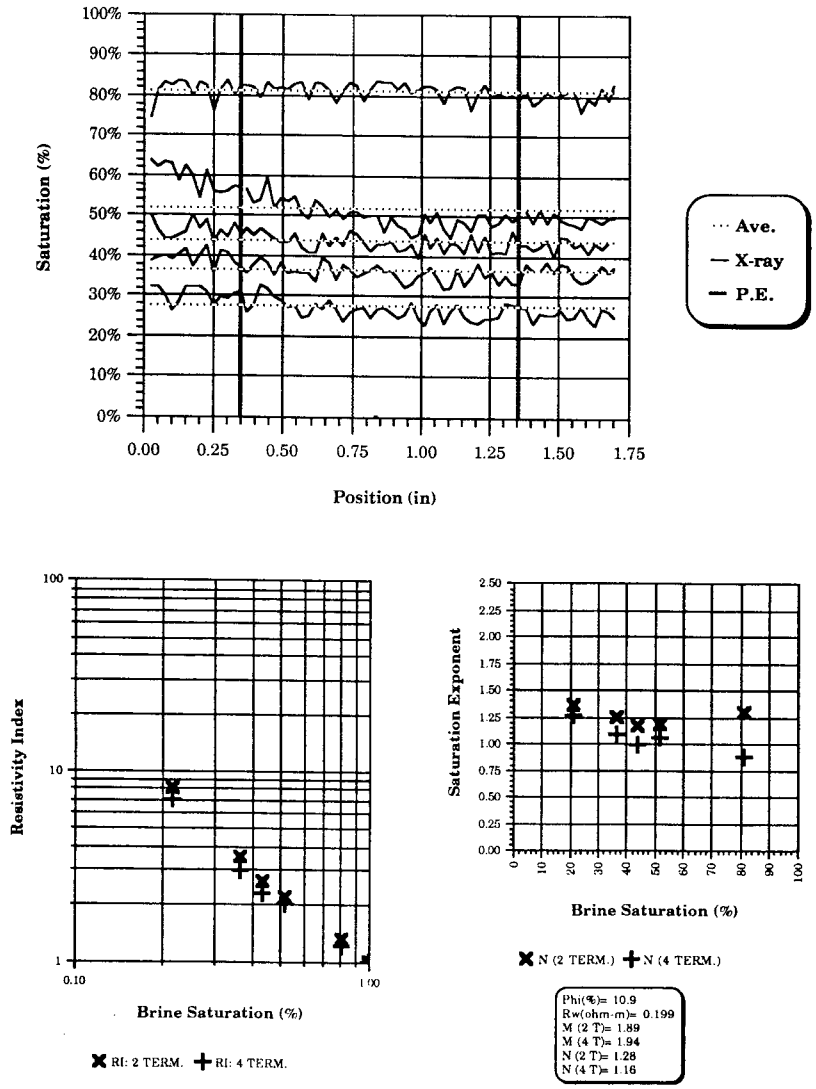

Figure 12: RI, N, and Sat. Distribution, Sample 7388.8, Porous Plate Desat.,24Hr.

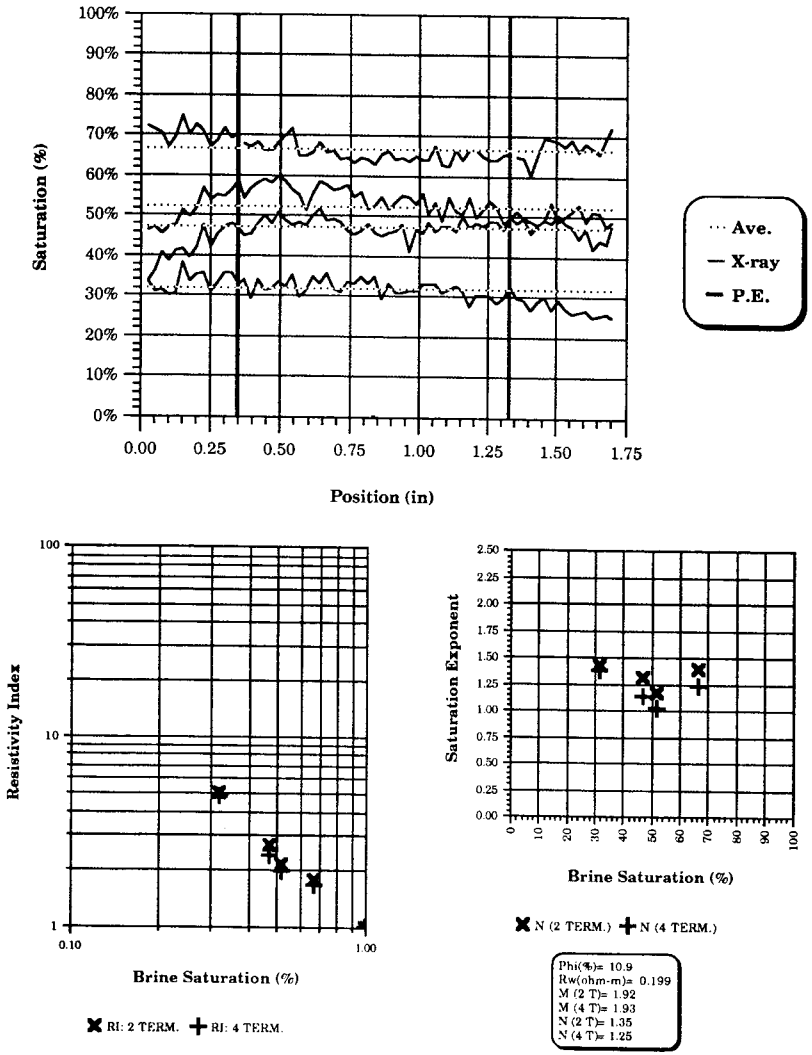

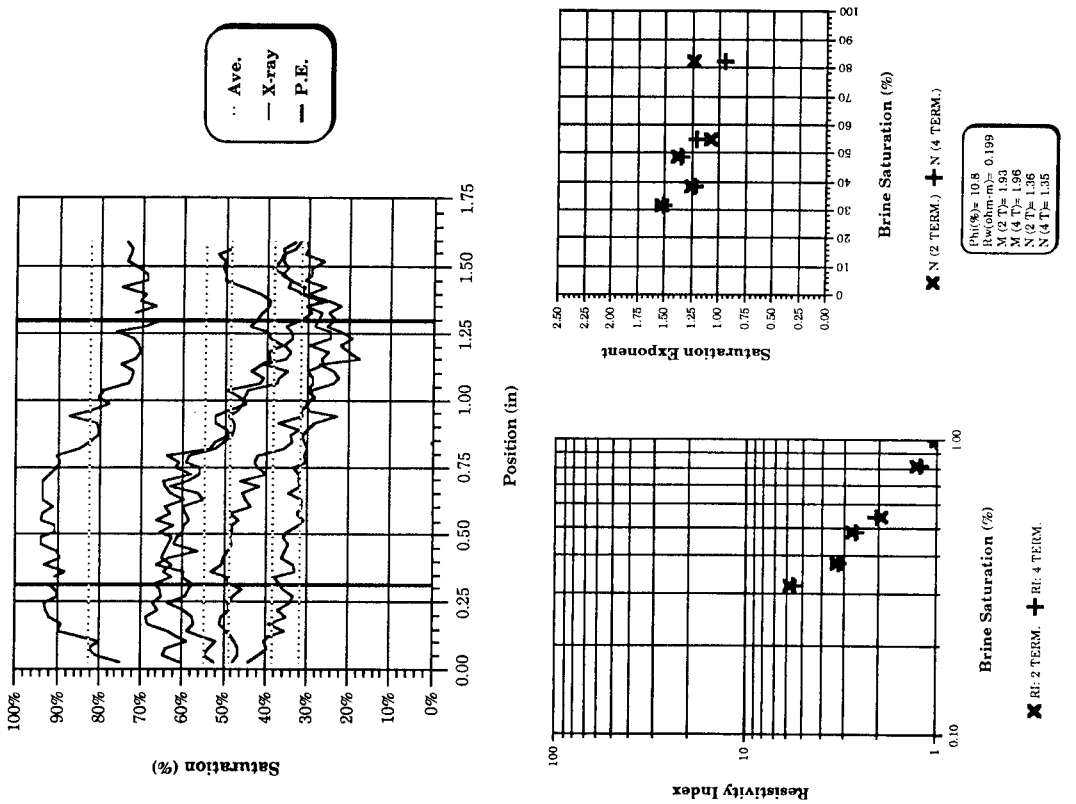

Figure 14: RI, N, and Sat. Distribution, Sample 7390.5, Porous Plate Desat.,24Hr.

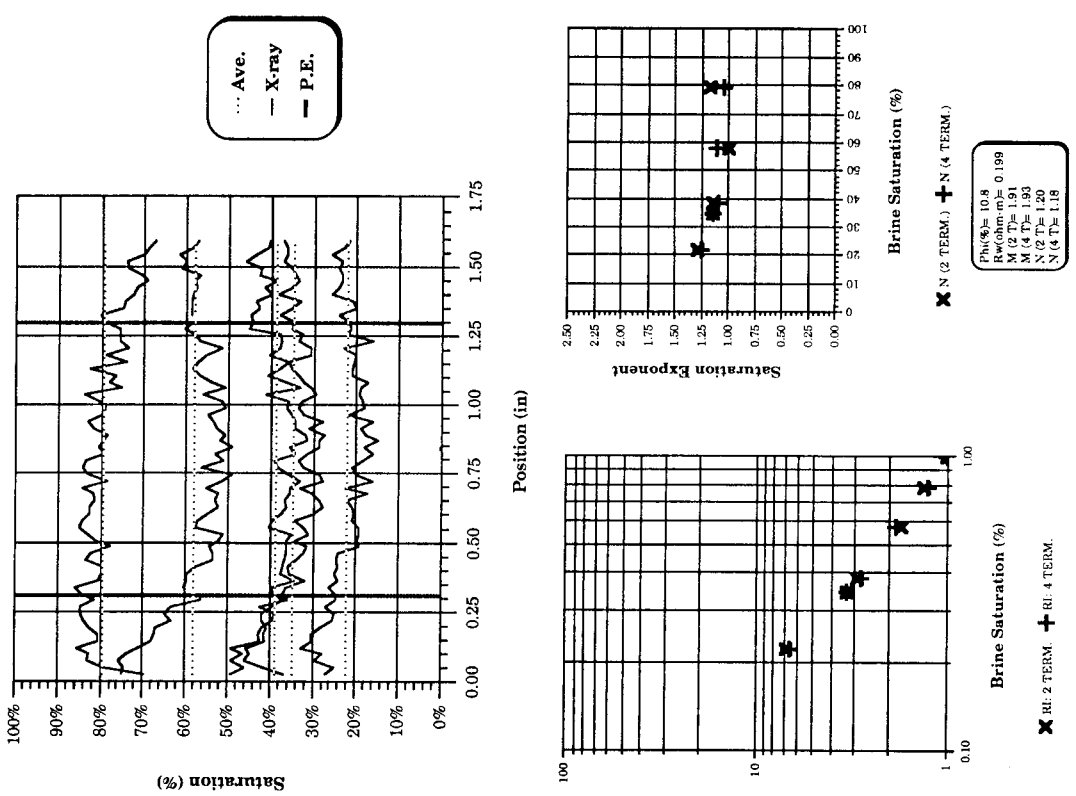

Figure 13: RI, N, and Sat. Distribution, Sample 7390.5, Cent. Desat.,24Hr.

Figure 15: RI, N, and Sat. Distribution, Enron S. Hogsback Well Sample 7127.5, Cent. Desat., 24 Hr. Equilibrium

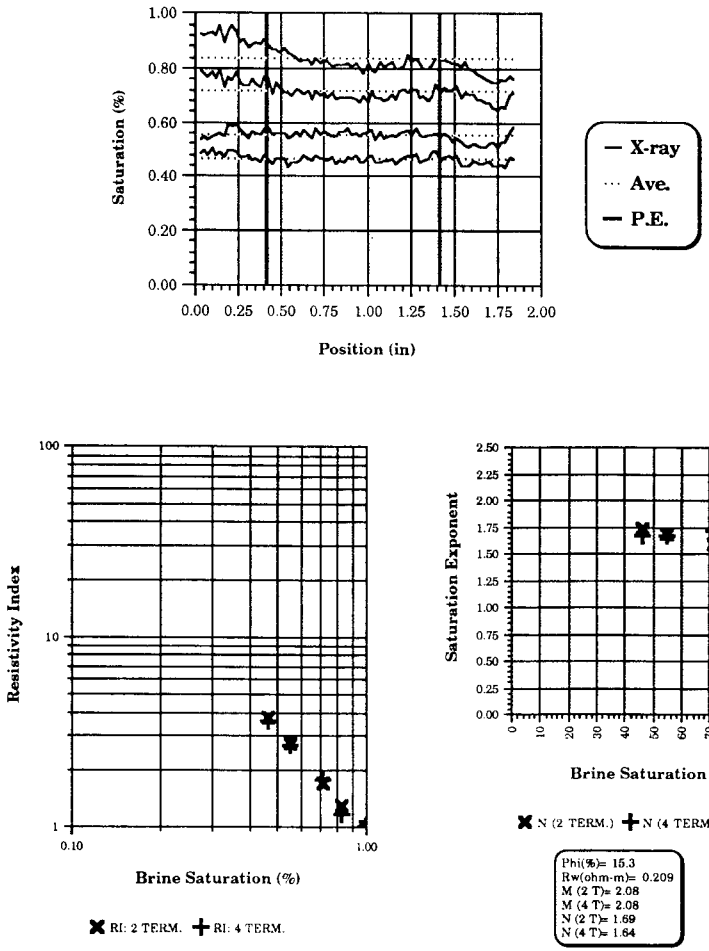

Figure 16: RI, N, and Sat. Distribution, Enron S. Hogsback Well Sample 7127.5, Porous Plate Desat., 24 Hr. Equilibrium

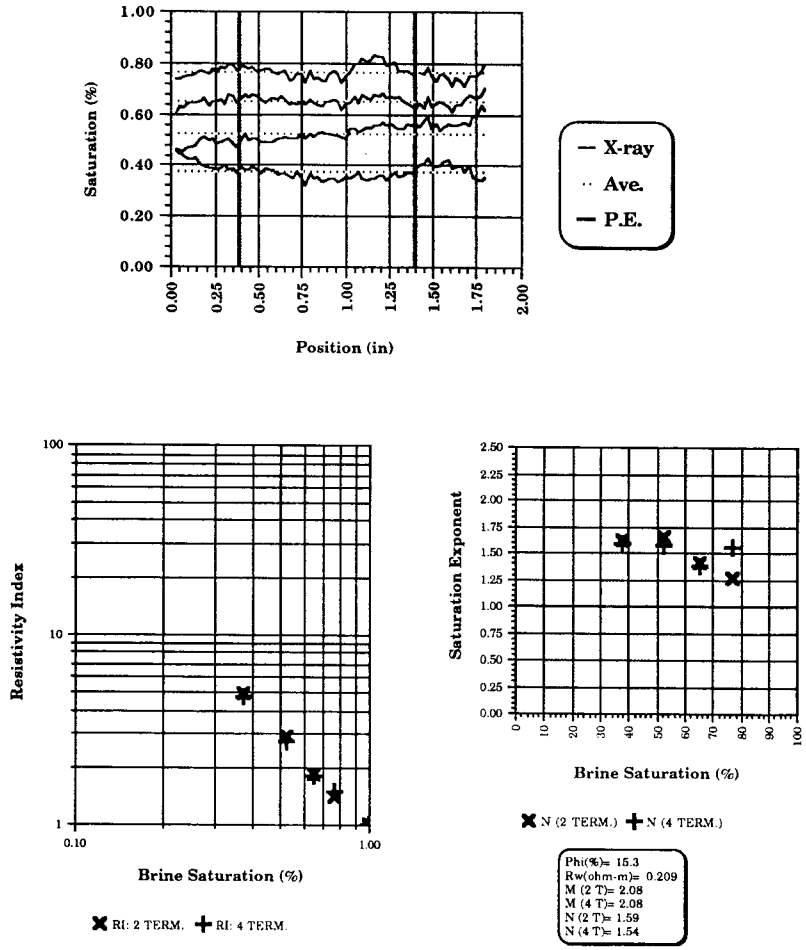

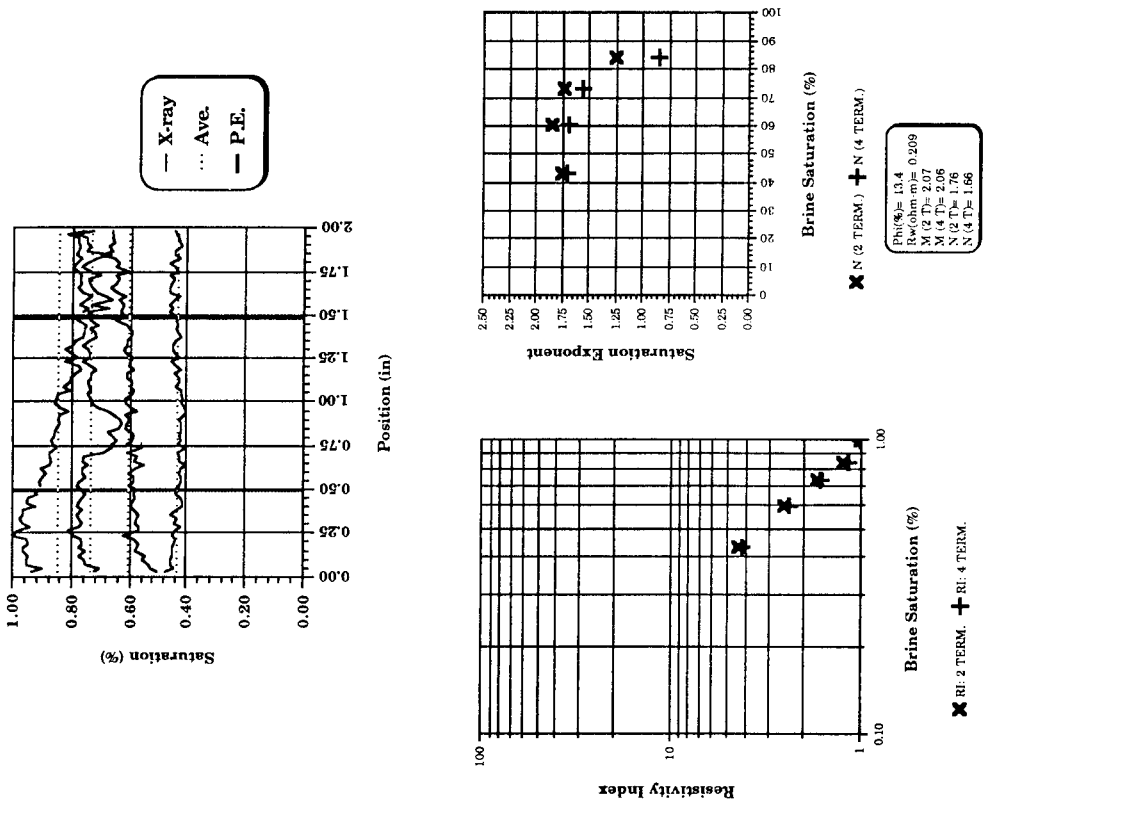

Figure 18: RI, N, and Sat. Distribution, Enron S. Hogsback Well
Sample 7114, Porous Plate Desat., 24 Hr. Equilibrium

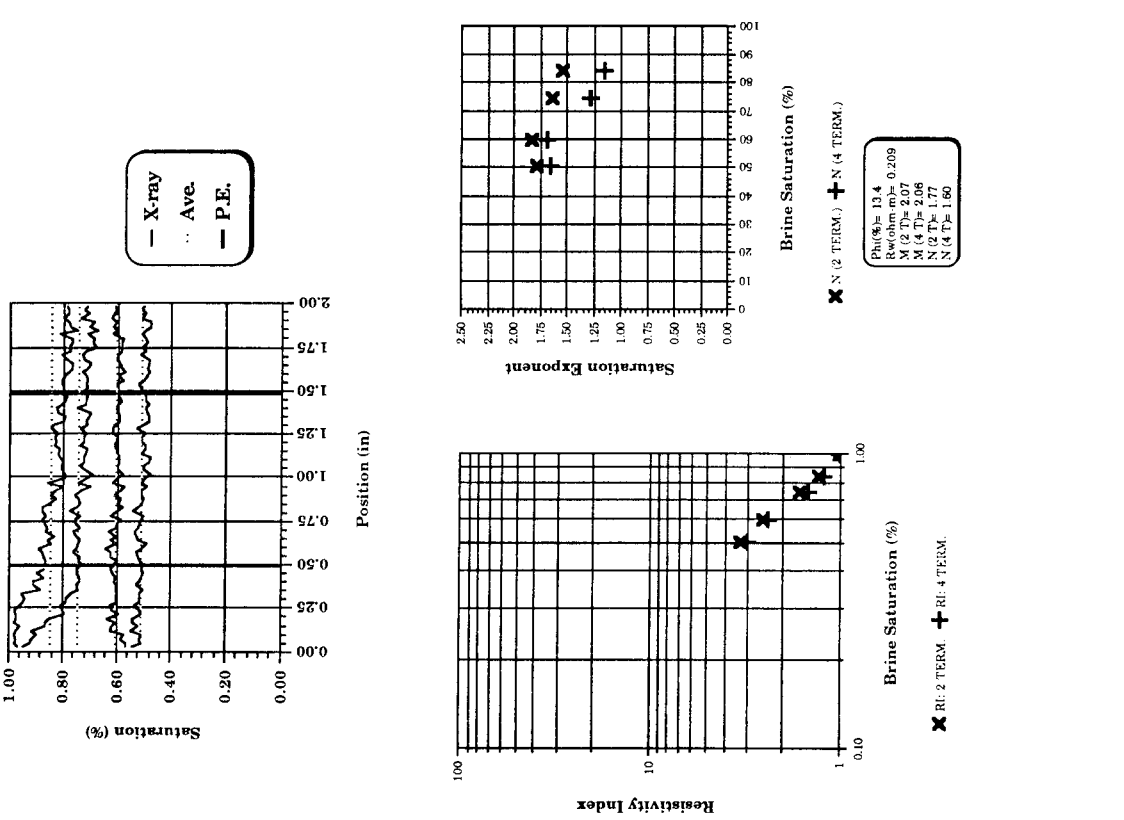

Figure 17: RI, N, and Sat. Distribution, Enron S. Hogsback Well
Sample 7114, Centrifuge Desat., 24 Hr. Equilibrium